

Cardiovascular Risk Factors Predict the Spatial Distribution of White Matter Hyperintensity

Soham Banerjee BS

Collaborators: Kevin S. King MD; Roderick W. McColl PhD; Anthony R. Whittemore MD,
PhD; Keith M. Hulsey PhD; Ronald M. Peshock MD

DISSERTATION

Presented to the Faculty of the Medical School

The University of Texas Southwestern Medical Center

In Partial Fulfillment of the Requirements

For the Degree of

DOCTOR OF MEDICINE WITH DISTINCTION IN RESEARCH

The University of Texas Southwestern Medical Center

Dallas

Cardiovascular Risk Factors Predict the Spatial Distribution of White Matter Hyperintensity

Abstract

Objectives: To identify the different spatial distribution of white matter hyperintensity (WMH) associated with specific risk factors and use this distribution to estimate the extent of risk factor associated WMH in an individual.

Materials and Methods: MRI brain images were obtained from 2066 healthy adult participants (858 males, 1208 females; mean age: 50) from a population based sample. An automated algorithm generated each participant's WMH distribution, registered onto the MNI-152 standard template. For univariate analysis, each risk factor group was compared to the non-risk factor group. Voxels in which WMH frequency was significantly higher ($p < 0.05$) in the risk factor group were mapped. Multivariate analysis consisted of subgroup analysis to minimize confounding of a risk factor on the others.

Results: 431891 MNI-space voxels comprised WMH distribution of the entire population. For univariate analysis, 23697 voxels (5.5%) of these voxels were exclusively associated with hypertension and were prevalent in the anterior frontal lobe. Similarly, 24637 voxels (5.7%) were exclusively associated with diabetes and were prevalent at the callososeptal interface. 7315 voxels (1.7%) were only associated with hypercholesterolemia and did not form a discrete spatial distribution. 282115 voxels (65.3%) were not associated with any of the specified risk factors. Multivariate results corroborated the univariate findings.

Conclusions: Each risk factor was associated with a different spatial distribution of WMH. Hypertension was associated with WMH in the anterior frontal lobe and diabetes was associated with WMH in the callososeptal interface.

Keywords: white matter hyperintensity; cardiovascular risk factor; voxel based morphometry; spatial analysis

Introduction

White matter hyperintensity (WMH) is brain white matter with high intensity on FLAIR and T2-weighted MRI. While its pathophysiology is incompletely understood, WMH is associated with certain cardiovascular risk factors, such as hypertension and diabetes (1-3). Hypercholesterolemia, conversely, has been shown to be associated with decreased WMH volume (4, 5). Normal aging is also an important contributor to increased WMH volume (6-8).

WMH has been considered a marker of end organ damage in the brain (7, 9). similar to microalbuminuria being a marker for end organ kidney damage in diabetes (10). However, given the independent effect of aging on total WMH volume, it would be import to identify whether a WMH lesion represents risk factor associated end organ brain injury or is related to aging.

The literature suggests that patients with cardiovascular risk factors may have different spatial distributions of WMH compared to individuals without these risk factors (11, 12). If there is a characteristic distribution of WMH associated with a particular cardiovascular risk factor, the finding of this distribution could indicate a more specific target for aggressive management. Our hypothesis is that cardiovascular risk factors (specifically hypertension, diabetes mellitus, and hypercholesterolemia) each have different spatial distributions of WMH.

The questions addressed in this study were: [1] is the spatial distribution of WMH different in individuals with a specified cardiovascular risk factor compared to that in individuals without the risk factor? [2] does the spatial distribution in individuals with the risk factor differ from that in individuals with other risk factors?

Materials and Methods

Experimental design

This cross-sectional study was Health Insurance Portability and Affordability Act compliant and had institutional review board approval. All data were obtained as part of a multi-ethnic, population-representative study of cardiovascular disease. This is the first study to analyze the spatial distribution of WMH using this cohort.

Each participant's MRI images were analyzed using an existing, automated algorithm to determine the location of voxels with WMH.

For univariate analysis, the population was divided into two groups depending on the presence of a risk factor. The prevalence of WMH in the two groups was compared at each voxel, and voxels in which WMH was significantly more prevalent in the risk factor group were determined creating a "spatial distribution map" for that risk factor. Figure 1 demonstrates the general process used for univariate analysis.

For multivariate analysis, each risk factor group was divided into four subgroups based upon the presence or absence of the other two risk factors. Each subgroup was compared against the population lacking the original risk factor and all voxels of WMH significantly more prevalent in the subgroup were identified. The statistically significant voxels common to all four subgroup analyses were considered to be associated with the original risk factor, independent of the other two risk factors. (See Figure 1)

Study Population

The study population consisted of 2066 participants who underwent brain imaging as part of the original population representative study. 1478 of these participants were recruited using population-based sampling. The remaining 588 participants consisted of relatives of the 1478 participants, chosen randomly from the original sample. (See Table 1)

MR Imaging

The images were acquired using a 3T MRI system (Achieva, Philips Medical Systems). An 8 channel phased array head coil was used. The 3D MP-RAGE (Magnetization-Prepared 180 Degrees Radio-Frequency Pulses and Rapid Gradient-Echo (13)) images were acquired with TR/TE = 9.6/5.8 msec, flip angle = 12°, SENSE factor = 2, field of view (FOV) = 260 x 260 mm, 2 mm slices spaced at 1 mm intervals, Rows x Cols x Slices = 288 x 288 x 140, and voxel size of 1 x 0.9 x 0.9 mm. The 2D FLAIR (Fluid Attenuated Inversion Recovery) images were acquired with TR/TE/TI = 11,000/130/2800 msec, ETL = 44, SENSE factor = 2, FOV = 250 x 250 mm, 4 mm slices with a 1 mm gap, Rows x Cols x Slices = 560 x 560 x 32, and voxel size of 5 x 0.45 x 0.45.

Identifying White Matter Hyperintensities and Registration to a Standard Brain Template

The automated WMH quantification method has been described elsewhere (14). Briefly, for each subject, a data derived threshold was applied to the FLAIR intensities to identify hyperintense white matter voxels. The resulting WMH masks formed a binary WMH map for each participant. The WMH masks were then registered onto the template MNI-152 atlas (Montreal Neurological Institute) in which one voxel corresponds with 1 mm³ in a standardized brain. All results reported in this study are derived from the MNI-152 space WMH maps and plotted on ICBM 152 nonlinear atlases (15). During review, two neuroradiologists assessed each

MRI and no evidence of other white matter disease, such as stroke or multiple sclerosis, was noted.

Risk Factors Definitions

A multidisciplinary committee as part of the original population based study developed criteria for assigning a participant to each risk factor group. Hypertension was defined as having an average systolic blood pressure ≥ 140 mmHg or an average diastolic blood pressure ≥ 90 mmHg from 3 separate visits or undergoing current treatment with antihypertensive medication. Diabetes mellitus was defined by self-report accompanied by use of anti-hyperglycemic medication, elevated serum glucose (fasting > 126 mg/dL [7.0 mmol/L] or non-fasting glucose > 200 mg/dL [11.1 mmol/L] (16). Hypercholesterolemia was defined as a fasting low-density lipoprotein cholesterol level greater than 160 mg/dL (4.1 mmol/L), non-fasting direct low-density lipoprotein cholesterol greater than 200 mg/dL (5.2 mmol/L), nonfasting total cholesterol level greater than 200 mg/dL (5.2 mmol/L), or use of statin medication.

Univariate Statistical Analysis

For each risk factor, the population was divided into two groups: those with the risk factor and those without it. For each group, the prevalence of WMH at each voxel was determined. Then the prevalence at each voxel was compared between the two groups using a nonparametric two-tailed permutation test (17). The permutation test was chosen over the chi square test and Z-test due to its superior accuracy when dealing with low proportions, as is seen in the prevalence of WMH. Additionally, permutation tests provide adequate power and low false positive rates for multiple comparison tests (18, 19). To perform this test, we created a program that pooled every voxel value across all participants and then randomly redistributed them into two subgroups, thus generating a permutation. The null hypothesis states that the

values of both groups are derived from the same distribution of values. If the alternative hypothesis (that the values of the group are derived from different distributions) were correct, randomly redistributing the values would generate a more extreme mean difference less than alpha percent of all permutations. The overall α was set at 0.05. 5000 permutations were performed for each statistical test. Every statistically significant voxel that was more prevalent in the risk factor group was mapped onto a standard template brain. Voxels that were only associated with one risk factor group, but not associated with the other two risk factor groups in univariate analysis, were isolated and mapped onto risk factor exclusive spatial distribution maps.

Multivariate Statistical Analysis

Each risk factor group was divided into four subgroups based upon their presence or absence of the other two risk factors, using multivariate risk stratified analysis (20).

For example, for hypertension, the hypertensive population was split into individuals with diabetes, without diabetes, with hypercholesterolemia, and without hypercholesterolemia. Each of these subgroups was compared with the normotensive population using permutation analysis like the one described for univariate analysis. The statistically significant voxels common to all four subgroups analysis were considered to be associated with hypertension, independent of the effects of diabetes and hypercholesterolemia.

For the majority of subgroups, the average age differed from the population mean substantially. Since age is an important contributor to the morbidity of each risk factor, this phenomenon was countered by employing scalar weighting of participants in the subgroup based upon age to achieve a mean age for the subgroup similar to the mean age of the population.

Results

Every participant in the study had WMH, with a median value of 1163 WMH voxels with quartiles 1 and 3 being 779 and 1908 voxels respectively.

The original sample of 1478 participants had a slightly lower mean age than the overall population (51 vs. 50 years). Additionally, the original sample had a slightly smaller percentage of females than the overall population (56% vs. 58%). The percentage of hypertensives was similar in both groups (47%). The percentage of diabetics in the original population was slightly greater (14% vs. 13%) as was the percentage of individuals with hypercholesterolemia (28% vs. 26%).

Univariate Results

Each risk factor had a spatial distribution distinct from the non-risk factor population's distribution and distinct from the other risk factors' distributions. Figures 3 and 4 contain the significant voxels for these tests mapped onto a standard brain template for each risk factor.

For the hypertensive subpopulation (including those with and without other risk factors), the total WMH distribution consisted of 370678 voxels (86.5% of the entire population's distribution of 428620 voxels). Similarly, the diabetic subpopulation's WMH distribution consisted of 241169 voxels (56.3%) and the hypercholesterolemia subpopulation's WMH distribution consisted of 292313 voxels (68.2%). Table 2 provides data about the number of *significant* voxels in various subgroups. (See Table 2)

Areas only associated with hypertension were located primarily in the anterior frontal lobe, especially in the deep and subcortical white matter. WMH specific to only diabetes was notably present along the midline brain. Since we did not expect to find midline brain WMH, the

original FLAIR images of ten randomly selected participants with suspected midline brain findings were reviewed by a neuroradiologist. The FLAIR images of all ten participants demonstrated WMH in the corpus callosum at the callososeptal interface. Additionally, hyperintensity findings were located in the septum pellucidum. (See Figure 2)

While voxels associated with hypercholesterolemia were widespread, there was no unique and discrete pattern associated with hypercholesterolemia (Figure 3). While previous literature has suggested that hypercholesterolemia is associated with a decreased volume of WMH in certain subgroups (4), our data contradicted this finding. The average participant with hypercholesterolemia had 2844 voxels of WMH, while the average participant without hypercholesterolemia had 1936 WMH voxels ($p < 0.0001$ in one tailed Mann Whitney U test). (See Figure 3)

All three risk factors were independently associated with WMH in the areas surrounding the frontal and posterior horns of the lateral ventricles. Additionally, all three risk factors had small yet sizable associated regions in the posterior brain, around the watershed zone between the middle cerebral and posterior cerebral arteries. These regions extended slightly into the occipital lobe, though outside this narrow zone, the occipital lobe did not demonstrate any risk factor associated areas.

Deep white matter regions lateral to the body of the lateral ventricles were less likely to be significantly associated with a risk factor. Regions posterior to the posterior horns of the lateral ventricles also demonstrated less association with a risk factor. The temporal lobe did not contain risk factor associated regions. Furthermore, subcortical WMH throughout the cerebral hemispheres was not associated with any risk factor. (See Figure 4)

Multivariate Results

For the multivariate analysis, there were 11729 statistically significant voxels common to all subgroups of hypertension. There were 20597 voxels common to all subgroups of diabetes and 5389 voxels common to all subgroups of hypercholesterolemia. Hypertension-common voxels were notably present in the frontal regions and absent from the midline brain. Diabetes-common voxels were notably present along the brain midline and absent from the frontal regions. Hypercholesterolemia-common voxels were not clustered in any discrete region. (See Figure 5)

Discussion

The results of the study show that risk factor populations do have different distributions of WMH than non-risk factor populations. WMH associated with hypertension, diabetes, and hypercholesterolemia shared common spatial territories, but each risk factor was also associated with different regions.

It has previously been established that cardiovascular risk factors are associated with increased WMH volumes; as a result, WMH is considered to be a marker for cerebrovascular injury in the brain and therefore risk factor associated end organ brain injury. In previous studies of stroke victims and elderly individuals, hypercholesterolemia has been shown to be associated with decreased volume of WMH, though our data, derived from community dwelling adults, do not support this finding (4). In the process of normal aging, WMH increases even when adjusted for risk factors (7). Our study focuses on the varying patterns of WMH with respect to cardiovascular risk factors, even against the background of age associated brain changes. Identifying the voxel patterns that are associated only with a specific cardiovascular risk factor

could allow a more specific assessment of the patient's extent of vascular injury or end organ brain injury from risk factors.

WMH associated with hypertension was especially abundant in the frontal lobe, which was not seen with diabetes or hypercholesterolemia. These areas were clustered around the watershed zone between territories covered by the anterior and middle cerebral arteries. In other studies of the impact of hypertension on the brain, pathologic changes were seen in the frontal lobe, supporting our findings (21). In these previous studies, hypertension was shown to be associated with smaller prefrontal cortices, increased frontal WMH volume, and executive dysfunction. Therefore, the evidence suggests that WMH found in the frontal lobe is significantly more likely to be associated with hypertension than other risk factors.

Hyperintensities linked to diabetes were uniquely present in the midline brain, corresponding to the corpus callosum at the callososeptal interface as well as in the septum pellucidum. Corpus callosum white matter lesions have been associated with traumatic brain injury and multiple sclerosis in previous case studies. However, other evidence has indicated that vascular injury might impact the corpus callosum. In a case review of patients with ischemic injury, lesions were found to be asymmetric and located in the medial aspect of the corpus callosum, similar to our statistical distribution for diabetes, a vascular disease (22). In another case study, diabetics were found to have decreased volumes of their corpora callosa (23). WMH in the callososeptal interface of diabetics could serve as a marker for diabetic white matter injury and additionally, corpus callosum injury could potentially present with clinical manifestations in patients with advanced diabetes. The clinical manifestations of corpus callosum injuries are varied, but they are associated with neuropsychiatric syndromes (24). The presence of

hyperintensities at the septum pellucidum on FLAIR may serve as a useful marker for diabetic brain injury.

Areas of WMH associated with all three risk factors were located adjacent to the anterior and posterior horns of the lateral ventricle. In previous pathological studies, the periventricular caps of WMH were associated with loss of ependymal lining, possibly secondary to local ischemia (25). As a result, our findings suggest that ependymal injury may be due to the vascular risk factors analyzed in our study.

Hypercholesterolemia was significantly associated with substantially less voxels of WMH than either hypertension or diabetes. Moreover, there were few sizable contiguous clusters of WMH associated with hypercholesterolemia. However, our results disagree with prior studies that suggest that hypercholesterolemia is associated with decreased volume of WMH.

The multivariate analysis confirmed the univariate results that showed that hypertension was significantly associated with the frontal lobe, independent of diabetes and hypercholesterolemia. Similarly, diabetes was significantly associated with the midline brain, independent of the hypertension and hypercholesterolemia. The multivariate data supports the conclusions of the univariate data for each risk factor and minimizes the issue of confounding due to the other two variables.

There are prior studies which attempt to explore the importance of spatial distribution of WMH with relationship to cardiovascular risk factors. DeCarli et al. investigated the hypothesis that vascular risk factors and age had stronger associations with periventricular WMH than deep WMH. They concluded that the arbitrary division of WMH into these anatomic groups did not yield any association with the risk factors they studied (12).

More recently, Rostrup et al. analyzed the distribution of WMH associated with vascular risk factors and performed their analysis on a voxel by voxel basis. For each voxel, they determined the strength of association between the probability of WMH at that voxel and the severity of the risk factor (11). However, their sample population was the LADIS study, a convenience sample drawn from multiple sites across Europe, in which participants were enrolled on the basis the presence of WMH on MRI. Their study consisted of 605 subjects with ages ranging between 65-84 with a mean age of 74.

Our study applies voxel based analysis to a large cohort of 2066 participants sampled from a single site study, population-based sample with an age range of 18 to 85 with a mean age of 50. This reduces the potential for referral bias and allows us to investigate the effects of risk factors in younger people. Our data suggest that WMH is present even in our younger and healthier cohort, potentially allowing the opportunity to intervene at an earlier age.

We also compared risk factors with each other, not just in comparison to a control population. Also, Rostrup's method consists of correlation analysis between the severity of a risk factor associated variable and the prevalence of WMH. This analysis provides less ability to detect effects caused by the long duration of a risk factor of mild severity. Given that most patients with a risk factor only have mild or moderate severity, correlation analysis may miss important findings. In contrast, our analysis does not evaluate the severity of a risk factor associated variable, but instead only evaluates for the risk factor's presence or absence.

Our study is limited by the possible effect of confounding bias, particularly in the univariate analysis. The multivariate analysis minimizes confounding due to the specified variables that were analyzed, due to its co-analysis of the variables. A further limitation is that our analysis determines a single time point association of voxels with risk factors and is not

prognostic of disease progression. As a result, our study can only determine association, not causation between risk factor and WMH.

In conclusion, our study demonstrated that each risk factor was associated with different spatial distributions of WMH: hypertension was associated with WMH in the anterior frontal lobe and diabetes was associated with WMH in the calloseseptal interface. Importantly, no a priori assumptions were made dividing the brain into functional or vascular territories; as a result the data are not influenced by divisions that may not hold significance to the underlying pathophysiology of WMH. Our results suggest that these cardiovascular risk factors are associated with different anatomic locations of end organ brain injury. Knowing the preferential associations of risk factors may allow increased specificity when assessing the extent of risk factor associated white matter injury in the brain. We would direct future studies to determine if aggressive treatment of individuals with risk factor characteristic WMH distribution leads to lower white matter lesion burden.

References

1. King KS, Chen KX, Hulsey KM, et al. White Matter Hyperintensities: Use of Aortic Arch Pulse Wave Velocity to Predict Volume Independent of Other Cardiovascular Risk Factors. *Radiology*. 2013;267(3):709-17.
2. Launer LJ. Epidemiology of white matter lesions. *Topics in Magnetic Resonance Imaging*. 2004;15(6):365-7.
3. Garde E, Mortensen EL, Krabbe K, et al. Relation between age-related decline in intelligence and cerebral white-matter hyperintensities in healthy octogenarians: a longitudinal study. *The Lancet*. 2000;356(9230):628-34.
4. Jimenez-Conde J, Biffi A, Rahman R, et al. Hyperlipidemia and Reduced White Matter Hyperintensity Volume in Patients With Ischemic Stroke. *Stroke*. 2010;41(3):437-42.
5. Sachdev P, Wen W, Chen X, Brodaty H. Progression of White Matter Hyperintensities in Elderly Individuals over 3 Years. *Neurology*. 2007;68(3):214-22.
6. Raz N, Yang Y, Dahle CL, Land S. Volume of White Matter Hyperintensities in Healthy Adults: Contribution of Age, Vascular Risk Factors, and Inflammation-Related Genetic Variants. *Biochim Biophys Acta*. 2012;1822(3):361-9.
7. King KS, Peshock RM, Rossetti HC, et al. Impact of Normal Aging versus Hypertension, Abnormal BMI and Diabetes on White Matter Hyperintensity Volume. *Stroke*. 2014.
8. Ylikoski A, Erkinjuntti T, Raininko R, et al. White matter hyperintensities on MRI in the neurologically nondiseased elderly Analysis of cohorts of consecutive subjects aged 55 to 85 years living at home. *Stroke*. 1995;26(7):1171-7.

9. DeBette S, Markus H. The clinical importance of white matter hyperintensities on brain magnetic resonance imaging: systematic review and meta-analysis. *BMJ: British Medical Journal*. 2010;341.
10. H Bennett P, Haffner S, Kasiske BL, et al. Screening and management of microalbuminuria in patients with diabetes mellitus: recommendations to the scientific advisory board of the national Kidney Foundation from an Ad Hoc Committee of the council on diabetes mel of the national kidney foundation. *American journal of kidney diseases*. 1995;25(1):107-12.
11. Rostrup E, Gouw AA, Vrenken H, et al. The Spatial Distribution of Age-Related White Matter Changes as a Function of Vascular Risk Factors—Results from the LADIS study. *Neuroimage*. 2012;60(3):1597-607.
12. DeCarli C, Fletcher E, Ramey V, et al. Anatomical Mapping of White Matter Hyperintensities (WMH): Exploring the Relationships between Periventricular WMH, Deep WMH, and Total WMH burden. *Stroke*. 2005;36(1):50-5.
13. Brant-Zawadzki M, Gillan GD, Nitz WR. MP RAGE: a Three-Dimensional, T1-Weighted, Gradient-Echo Sequence--Initial Experience in the Brain. *Radiology*. 1992;182(3):769-75.
14. Hulsey KM, Gupta M, King KS, et al. Automated Quantification of White Matter Disease Extent at 3 T: Comparison with Volumetric Readings. *J Magn Reson*. 2012;36(2):305-11.
15. Fonov V, Evans A, McKinsty R, et al. Unbiased nonlinear average age-appropriate brain templates from birth to adulthood. *NeuroImage*. 2009;47:S102.

16. Report of the Expert Committee on the Diagnosis and Classification of Diabetes Mellitus. *Diabetes Care*. 1997;20:1183-97.
17. Chihara LM, Hesterberg TC. *Permutation Tests. Mathematical Statistics with Resampling* and R. Hoboken, NJ: John Wiley & Sons; 2011:31-41.
18. Camargo A, Azuaje F, Wang H, Zheng H. Permutation - Based Statistical Tests for Multiple Hypotheses. *Source Code for Biology and Medicine* [serial online]. October 21, 2008 2008;3.
19. Nichols TE, Holmes AP. Nonparametric permutation tests for functional neuroimaging: a primer with examples. *Human brain mapping*. 2002;15(1):1-25.
20. Hayward RA, Kent DM, Vijan S, Hofer TP. Multivariable risk prediction can greatly enhance the statistical power of clinical trial subgroup analysis. *BMC medical research methodology*. 2006;6(1):18.
21. Raz N, Rodrigue KM, Acker JD. Hypertension and the Brain: Vulnerability of the Prefrontal Regions and Executive Functions. *Behav Neurosci*. 2003;117(6):1169-80.
22. Frieze S, Bitzer M, Freudenstein D, et al. Classification of Acquired Lesions of the Corpus Callosum with MRI. *Neuroradiology*. 2000;42(11):795-802.
23. Chen ZY, Li JF, Sun J, Ma L. [Changes in Subcortical White Matter and Corpus Callosum Volumes in Patients with Type 2 Diabetes Mellitus]. *Zhongguo Yi Xue Ke Xue Yuan Xue Bao. Acta Academiae Medicinae Sinicae*. 2013;35(5):503-14.
24. Georgy B, Hesselink J, Jernigan T. MR Imaging of the Corpus Callosum. *AJR*. 1993;160(5):949-55.

25. Leifer D, Buonanno FS, Richardson EP. Clinicopathologic Correlations of Cranial Magnetic Resonance Imaging of Periventricular White Matter. *Neurology*. 1990;40(6):911.

Table 1: Study Population Demographics

		Hypertension	Diabetes	Hypercholesterolemia	Total Population
Number of participants		962	269	567	2066
Sex					
	Male	377	123	258	858
	Female	585	146	309	1208
Race					
	Non-Hispanic White	269	60	236	750
	Non-Hispanic Black	582	153	252	975
	Hispanic	93	46	67	292
	Other	18	10	12	49
Mean Age		54	55.3	55	50.1
Mean Systolic Blood Pressure		143.1	139.1	134	131
Mean Diastolic Blood Pressure		84.6	81.5	80.5	80.4
Mean Hemoglobin A1C		5.9	7.6	5.9	5.7
Mean Total Cholesterol		192	185.2	208.7	194

Table 2: Numbers of Statistically Significant Risk Factor Associated Voxels in Univariate Analysis

	Number of Voxels	Percent of Total WMH Distribution
Total Distribution of WMH Across Study Population	431891	100%
WMH present in ≥ 10 participants	86719	20.1%
Hypertension Associated ^a	62877	14.6%
Diabetes Associated	60906	14.1%
Hypercholesterolemia Associated	33427	7.7%
Hypertension Associated Only ^a	23697	5.5%
Diabetes Associated Only	24637	5.7%
Hypercholesterolemia Associated Only	7315	1.7%
Associated with all three risk factors	15956	3.7%
No association with any risk factor	282115	65.3%

^a “Hypertension associated” refers to all voxels associated with hypertension. “Hypertension associated only”, refers to all voxels associated with hypertension that were not associated with either diabetes or hypercholesterolemia.

Figure Captions:

Figure 1: Overall Study Design

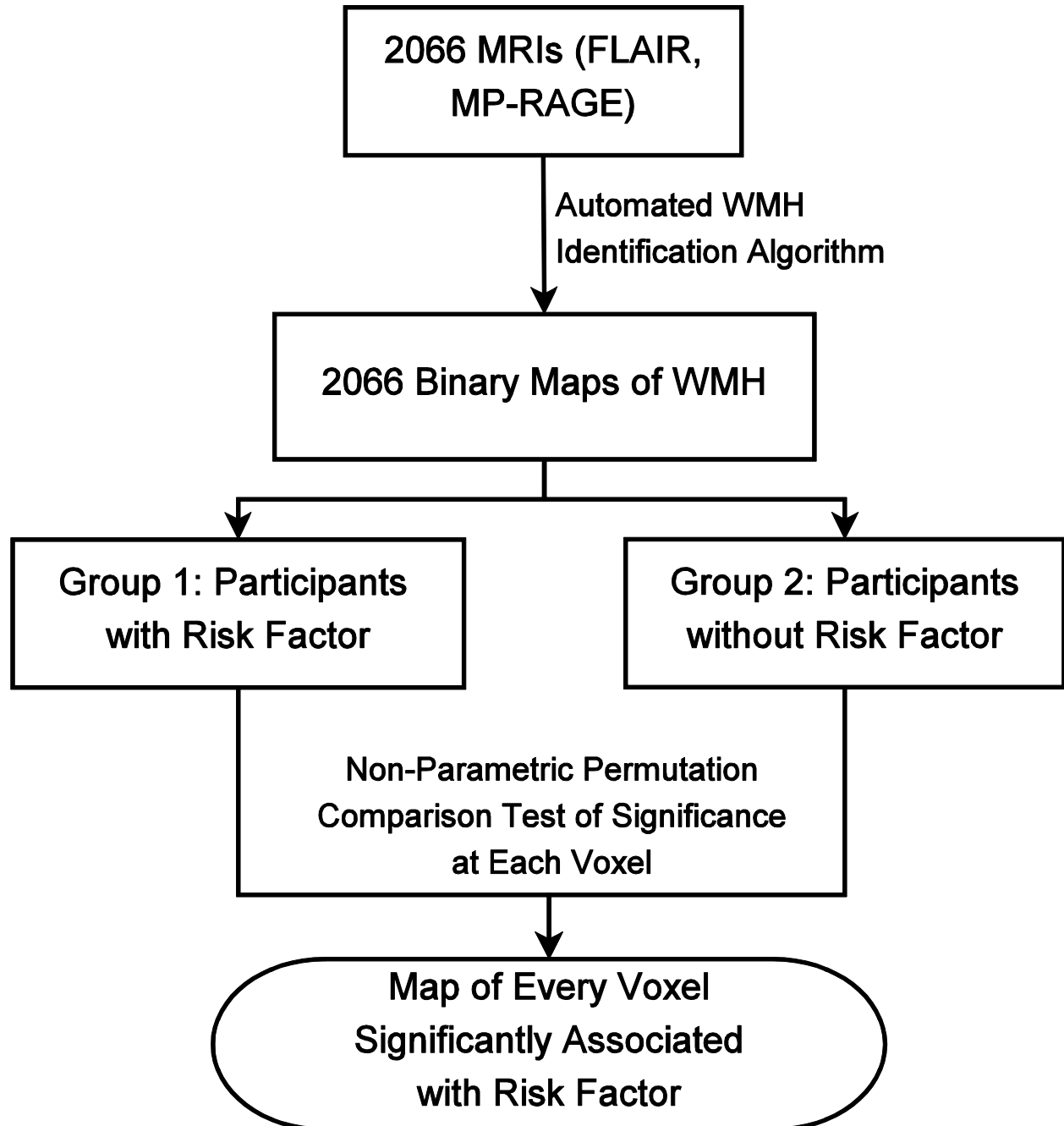


Figure 2: FLAIR MRI of participant with diabetes demonstrating WMH in the corpus callosum at the callososeptal interface and hyperintensity in the septum pellucidum.

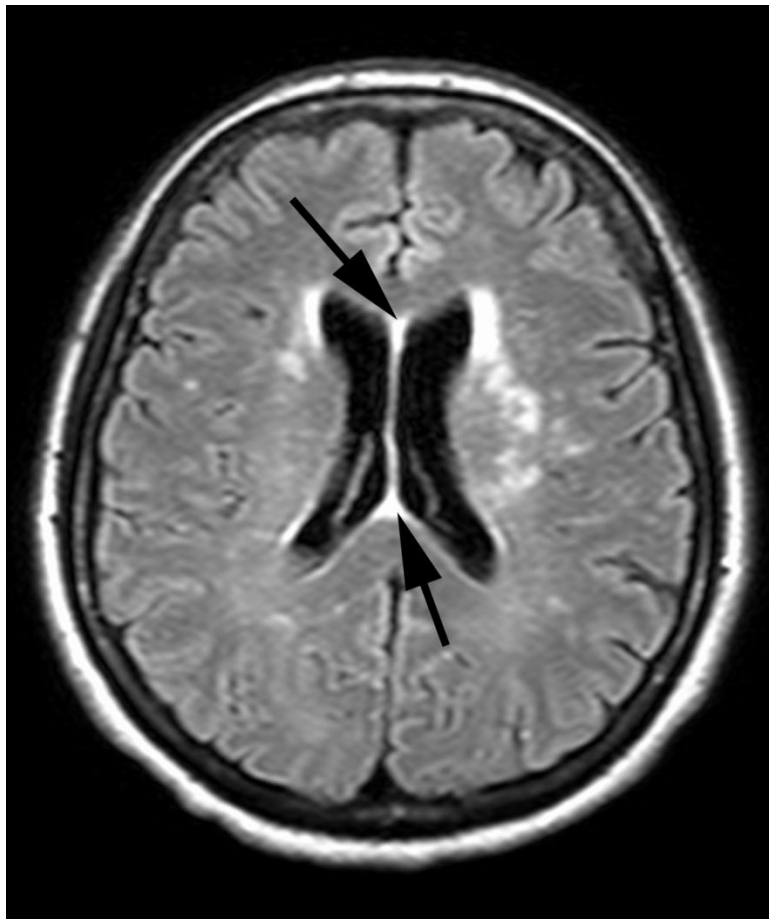


Figure 3: WMH Regions Exclusively Associated with One Risk Factor in Univariate Analysis.

Statistical Maps on a standardized brain template showing voxels that are only associated with

Left Column) hypertension, Middle Column) diabetes, and Right Column) hypercholesterolemia.

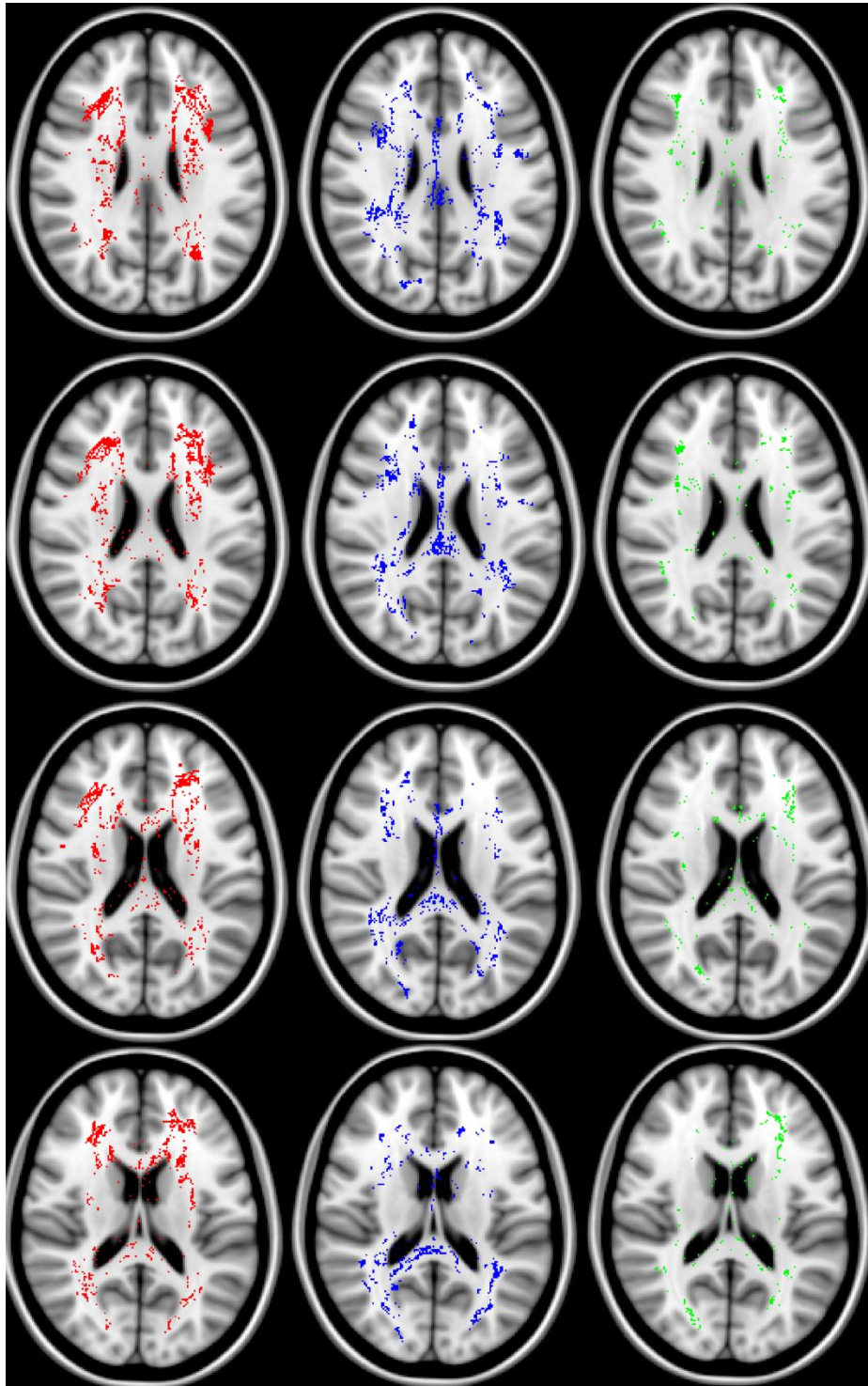


Figure 4: WMH regions associated with all three risk factors (left) and regions associated with no risk factor (right).

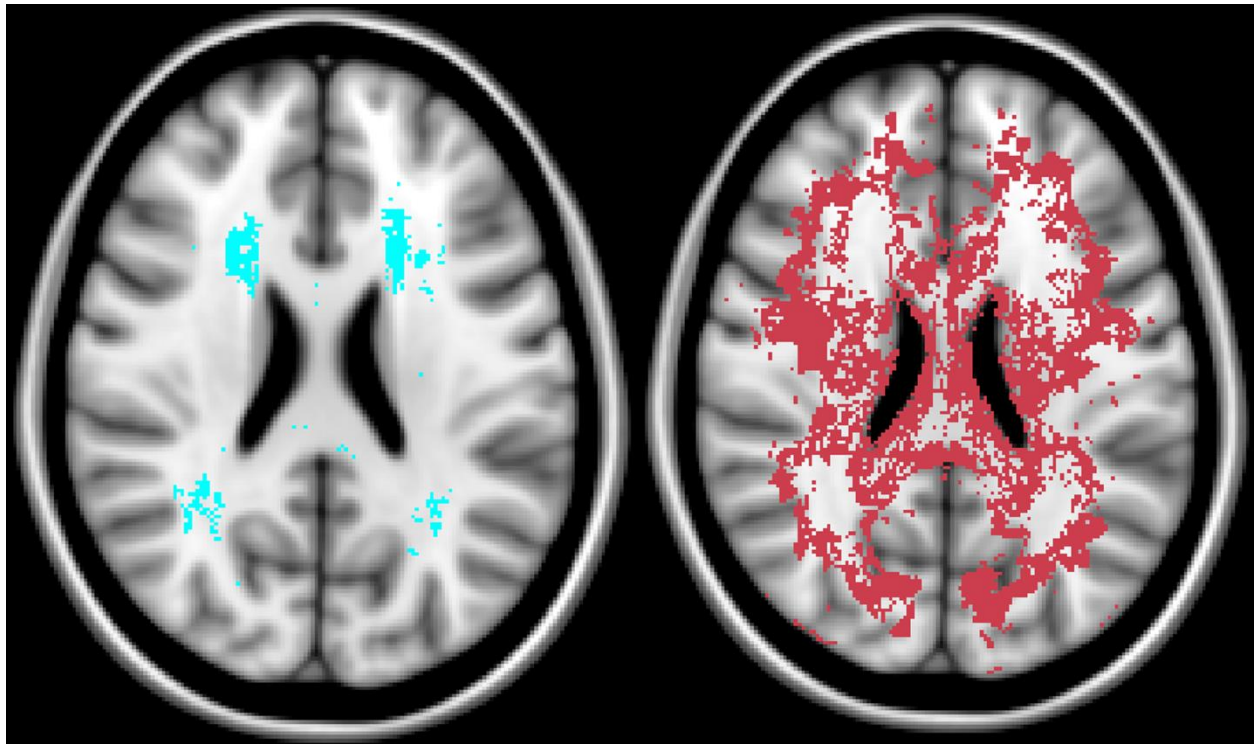


Figure 5: Multivariate Analysis Statistical Maps. Statistical maps on a standardized brain for voxels independently associated with hypertension (left) and diabetes (right). Notably, hypertension is independently associated with frontal brain regions, while diabetes is independently associated with midline structures.

